NASA Technical Memorandum 101302

A Transversely Isotropic Thermoelastic Theory

S.M. Arnold
Lewis Research Center
Cleveland, Ohio

Corrected Copy

November 1989

NASA

A TRANSVERSELY ISOTROPIC THERMOELASTIC THEORY

S. M. Arnold
National Aeronautics and Space Administration
Lewis Research Center
Cleveland, Ohio 44135

ABSTRACT

A continuum theory is presented for representing the thermoelastic behavior of composites that can be idealized as transversely isotropic. This theory is consistent with anisotropic viscoplastic theories being developed presently at NASA Lewis Research Center. A multiaxial statement of the theory is presented, as well as plane stress and plane strain reductions. Experimental determination of the required material parameters and their theoretical constraints are discussed. Simple homogeneously stressed elements are examined to illustrate the effect of fiber orientation on the resulting strain distribution. Finally, the multiaxial stress – strain relations are expressed in matrix form to simplify and accelerate implementation of the theory into structural analysis codes.

INTRODUCTION

Historically, the study of the mechanical behavior of fiber reinforced composite materials has been approached from two viewpoints, the microscopic and macroscopic. The microscopic view considers the constituents (fiber/matrix) separately, addressing in detail the interaction between individual fibers and surrounding matrix and the behavior at the fiber – matrix interface. Alternatively, the macroscopic approach considers the composite to be a material in its own right, (continuum), with its own experimentally measurable properties specified for the composite as a whole. This continuum approach provides a relatively efficient framework for the prediction of observed macroscopic deformation behavior. Extensive research into both the micro and macroscopic viewpoints has been undertaken (e.g.[1,2]).

Here, a continuum theory is presented for representing the thermoelastic behavior of composites that can be idealized as a homogeneous continua with locally definable directional characteristics. Although it is presumed here that a single preferential (fiber) direction is identifiable at each material point, thus admitting the idealization of local transverse isotropy, the theory is extendible to account for two (or more) identifiable preferential directions.

As indicated in [3], homogenization of textured materials (e.g composites) and applicability of continuum mechanics depends relatively upon characteristic structural dimensions, the severity of gradients (i.e. stress, temperature, etc.), and the relative scale and periodicity of the internal structure of the material. Examination of these conditions reveals that for many anticipated aerospace applications of composites, the formulation of continuum based theories is justified.

The objective of this study is the development of a transversely–isotropic thermoelastic theory which is consistent with present, continuum–based, anisotropic viscoplastic theories. Therefore the present work follows closely the earlier work of Spencer [2,4] and Robinson [3,5], and relies heavily upon invariant theory and the existence of a strain and complementary energy potential in the formulation of the constitutive equations. Major contributions of this study are 1) the recasting of earlier work in terms of physically meaningful total stress invariants, 2) discussion of a transversely isotropic multiaxial thermal strain tensor, 3) identification of a correspondence between plane stress and plane strain for a transversely isotropic material and 4) specification of an experimental program for the complete determination of the required elastic constants as well as a discussion of the theoretical restrictions on these parameters.

This study begins with the multiaxial statement of the theory, followed by the plane stress and plane strain simplifications. Experimental determination of the required material parameters and their theoretical constraints are then discussed. Simple applications are then employed to illustrate the capability of the theory in representing transversely isotropic thermoelastic behavior.

MULTIAXIAL STATEMENT OF THE THEORY

Here constitutive equations are given for a linear hyperelastic solid reinforced by a single family of fibers, i.e. a locally transversely isotropic material. Given a hyperelastic material the stress and strain components are related through a normality structure utilizing either a strain energy or complementary energy function [2,6], i.e.

$$\sigma_{ij} = \frac{\partial W}{\partial \epsilon_{ij}} \tag{1}$$

and

$$\epsilon_{ij} = \frac{\partial \Omega}{\partial \sigma_{ij}} \tag{2}$$

where

$$W = W(\epsilon_{ij}) \tag{3}$$

and

$$\Omega = \Omega(\sigma_{ij}) \tag{4}$$

Here σ_{ij} denotes the components of (Cauchy) stress, ϵ_{ij} the components of infinitesimal mechanical strain.

Transversely isotropic material symmetry is included in the potentials of equations (3) and (4) by introducing a directional tensor $d_i d_j$, for example:

$$W = W(\epsilon_{ij}, d_i d_j)$$

and

$$\Omega = \Omega(\sigma_{ij}, d_i d_j)$$

where now W and Ω depend not only upon ϵ_{ij} and σ_{ij}, respectively at a point but also upon the local fiber direction. The symmetric tensor $d_i d_j$ is formed by a self product of the unit vector d_i denoting the local fiber direction, as the sense of d_i is immaterial.

As W and Ω each depend on two symmetric second order tensors, form invariance (objectivity) requires that they depend only on certain invariants and invariant products of their respective tensorial arguments (i.e., an integrity basis). The integrity basis, for a function comprised of two symmetric second order tensors, has ten invariants [7]. A subset consisting of four invariants (I_1, I_2, I_4, I_5) of the irreducible set of invariants is used, as d_i is a unit vector and we desire W and Ω only to be quadratic functions (so the resulting stress strain relations are linear). Assuming a polynomial representation, the potential functions may be expressed as follows:

$$W(\epsilon_{ij}, d_i d_j) = A'P'_1 + B'P'_2 + C'P'_3 + D'P'_4 + E'P'_5 \tag{5}$$

and

$$\Omega(\sigma_{ij}, d_i d_j) = A\,P_1 + B\,P_2 + C\,P_3 + D\,P_4 + E\,P_5 \tag{6}$$

where

$$P_1 = I_1^2$$

$$P_2 = I_2 - I_5 + 1/4(I_4^2 - 9I_1^2 + 6I_1I_4)$$

$$P_3 = I_5 - I_4^2 \qquad (7)$$

$$P_4 = I_4^2$$

$$P_5 = I_1I_4$$

and

$$I_1 = \sigma_{ii}/3$$

$$I_2 = 1/2\ \sigma_{ij}\ \sigma_{ji}$$

$$I_4 = d_id_j\ \sigma_{ji} \qquad (8)$$

$$I_5 = d_id_j\sigma_{jk}\sigma_{ki}$$

An analogous set of invariants to those in equations (7) and (8) is chosen for W, i.e. $P_1',P_2',\ldots,P_5'$ and I_1',I_2',I_4',I_5', by replacing σ_{ij} by ϵ_{ij} in equations (7) and (8).

The subset of total stress invariants employed in (7) are similar to those utilized by Robinson and Duffy [3] for the corresponding deviatoric invariants. These invariants correspond physically to ; P_1 – the square of the mean (hydrostatic) stress state, P_2 – the square of the maximum transverse shear stress , P_3 – the square of the maximum longitudinal shear stress , P_4 – the square of the normal stress in the local fiber direction, and P_5 – the product of the mean and normal stress in the local fiber direction. Figure 1 defines the coordinate system and P_2,P_3 and P_4 schematically.

Substituting equations (5) – (8) into equations (3) and (4) result in the following linear elastic stress strain relations[1].

$$\sigma_{ij} = 1/6\{ (4A'-9B') I_1' + (3B' + 2E')I_4' \} \delta_{ij} + 1/2\{(3B' + 2E')I_1' + [B'+4(D'-C')]I_4' \} d_i d_j + B'\epsilon_{ij} + (C' - B') a_{ij}' \quad (9)$$

and

$$\epsilon_{ij} = 1/6\{ (4A-9B) I_1 + (3B + 2E)I_4 \} \delta_{ij} + 1/2\{(3B + 2E)I_1 + [B + 4(D -C)]I_4 \} d_i d_j + B\sigma_{ij} + (C - B) a_{ij} \quad (10)$$

where

δ_{ij} – denotes the Kronecker delta function

$a_{ij} = d_i \sigma_{jk} d_k + d_k \sigma_{ki} d_j$

$a_{ij}' = d_i \epsilon_{jk} d_k + d_k \epsilon_{ki} d_j$

Clearly equations (9) and (10) posses identical form; the coefficients and invariants, however are distinctly different. The unprimed coefficients A,B,C,D and E and their primed counterparts may be associated with more physical parameters (e.g. Young's modulus and Poisson ratio) by conducting various thought experiments. For example consider the four stress states depicted in figure 2, given a preferred direction d_i along the 2 axis, i.e. d=(0,1,0).

[1]The appendix contains identical expressions to those of (9) and (10), yet written in matrix notation for easy implementation into structural analysis codes.

From these states of stress (tests), it is easily shown that

test a)

$$B = \epsilon_{13}/\sigma_{13} = 1/2G_T \tag{11}$$

test b)

$$C = \epsilon_{12}/\sigma_{12} = 1/2G_L \tag{12}$$

test c)

$$2/9(A + 9D + 3E) = \epsilon_{22}/\sigma_{22} = 1/E_L \tag{13}$$

$$-1/9(2A + 3E)E_L = -\epsilon_{11}/\epsilon_{22} = \nu_L \tag{14}$$

and

test d)

$$2(A/9 + B/4) = \epsilon_{11}/\sigma_{11} = 1/E_T \tag{15}$$

$$\frac{-(4A - 9B)}{4A + 9B} = -\epsilon_{22}/\epsilon_{11} = \nu_T \tag{16}$$

$$-2(A/9 + E/6)E_T = -\epsilon_{33}/\epsilon_{11} = \nu_L' \tag{17}$$

Where

G_T – Shear modulus (transverse) for the plane of isotropy

G_L – Shear modulus (longitudinal) for a plane normal to the plane of isotropy.

E_T – Young's modulus (transverse) in the plane of isotropy.

E_L – Young's modulus (longitudinal) normal to the plane of isotropy.

ν_T – Poisson's ratio (transverse) that characterizes the transverse strain reduction in the plane of isotropy due to a tensile stress in the same plane.

ν_L – Poisson's ratio (longitudinal) that characterizes the transverse strain reduction in the plane of isotropy due to a tensile stress in a direction normal to it.

ν_L'– Poisson's ratio that characterizes the strain reduction normal to the plane of isotropy due to a tensile stress in the plane of isotropy.

Solving equations (13) thru (17) we find

$$A = \frac{9}{4}\left[\frac{(1-\nu_T)}{E_T}\right]$$

$$B = 1/2G_T$$

$$C = 1/2G_L \qquad (18)$$

$$D = (1+2\nu_L)/2E_L + (1-\nu_T)/4E_T$$

$$E = -3\{(1-\nu_T)/2E_T + \nu_L/E_L\}$$

and

$$2G_T = E_T/(1+\nu_T)$$

$$\nu_L' = \nu_L E_T/E_L$$

Note that the five independent constants are chosen to be E_L, E_T, ν_L, ν_T and G_L. A similar process can be repeated to obtain the primed coefficients in terms of these five independent physical parameters, they are:

$$A' = \frac{9}{4}\left\{E_T E_L/\left[E_L(1-\nu_T) - 2E_T\nu_L^2\right]\right\}$$

$$B' = 2G_T$$

$$C' = 2G_L \qquad (19)$$

$$D' = E_L\{1 + E_T(1-2\nu_L)^2/[2(E_L(1-\nu_T) - 2E_T\nu_L^2)]\}/2$$

$$E' = -3\{E_T E_L(1-2\nu_L)/[E_L(1-\nu_T) - 2E_T\nu_L^2]\}/2$$

Therefore, the stress–strain relations of (9) and (10) may be expressed either in terms of the nonphysical coefficients A,B,C,D and E, or alternatively in terms of the five independent physical parameters discussed above.

Agreement between the present work and earlier work by Spencer [4] is evident, provided appropriate substitutions are made for the coefficients in equation (9) prior to comparison of the strain energy formulations. Additionally, a direct comparison with Lekhnitskii's [8] work can be made when the physical parameters expressed in (18) are inserted into equation (10) and the preferred direction is assumed to be d=(0,0,1). Further, with appropriate substitution of equations (18) and (19) into (9) and (10), and considering conditions of isotropy, i.e.

$$E = E_L = E_T\,; \quad \nu = \nu_L = \nu_T \quad \text{and} \quad d_i d_j = \delta_{ij}/3 \tag{20}$$

the classical isotropic linear elastic stress – strain relations are obtained.

The transversely isotropic stress–strain relations given above may be extended to include the effect of temperature by applying the traditional assumption of the additive nature of mechanical and thermal strain, i.e.

$$e_{ij} = \epsilon_{ij} + \epsilon^t_{ij} \tag{21}$$

where

e_{ij} – total strain

ϵ_{ij} – mechanical strain

and the multiaxial thermal strain is assumed to have the following form

$$\epsilon^t_{ij} = [(\alpha_L - \alpha_T) d_i d_j + \delta_{ij}\alpha_T]\,\Delta T \tag{22}$$

where α_L – characterizes the thermal expansion normal to the plane of isotropy

α_T – characterizes the thermal expansion in the plane of isotropy

$\Delta T = T_2 - T_1$; T_1, T_2 are two distinct temperatures

A similar expression to that of (22) was derived by Chadwick and Seet [9] from the Helmhotz free energy for a heat conducting elastic transversely isotropic material. There it was also shown that such a form satisfies thermodynamic restrictions.

Again, imposing the conditions of isotropy ($\alpha=\alpha_L=\alpha_T$) it is evident that (22) reduces to

$$\epsilon_{ij}^{t} = \delta_{ij}\alpha\,\Delta T \tag{23}$$

the classical isotropic thermal strain tensor. Equation (23) is restricted to an isotropic continuum, as it implies that a change in temperature causes *only* a change in volume. This is not necessarily the case in (22), in that for an off axis fiber orientation a change in shape (shear) will occur with a change in temperature. An example of this is provided in a later section.

TWO DIMENSIONAL SIMPLIFICATION

Here, simplification of the multiaxial linear thermoelastic stress – strain relations of (21), in which equations (10) and (22) are incorporated, is made to that of plane stress and plane strain. For convenience equations (18), representing the relationship between physical and nonphysical parameters are substituted into (10). Plane stress, in the plane of isotropy (see figure 3), requires that

$$T_i = \sigma_{ij}n_j = 0$$

while plane strain requires

$$\exists_i = e_{ij}n_j = 0$$

where T_i and $\exists_i$ represent the stress and strain traction, respectively. If the local fiber direction (d_i) and n_j (indicating the directionality of the plane stress or strain assumption) are defined as,

$$\begin{aligned} d_1 &= \cos\theta & n_1 &= 0 \\ d_2 &= \sin\theta & n_2 &= 0 \\ d_3 &= 0 & n_3 &= 1 \end{aligned}$$

the following expressions relating the nonzero stress and strain components are obtained.

Plane Stress:

$$e_{11} = \sigma_{11}/E_T - \nu_L\sigma_{22}/E_L + [1/2G_L - 1/E_T - \nu_L/E_L](2\sigma_{11}\cos^2\theta + 2\sigma_{12}\cos\theta\sin\theta) + [1/E_T + (1+2\nu_L)/E_L - 1/G_L](\sigma_{11}\cos^2\theta + \sigma_{22}\sin^2\theta + 2\sigma_{12}\cos\theta\sin\theta)\cos^2\theta + [\alpha_T + (\alpha_L - \alpha_T)\cos^2\theta]\Delta T \quad (24)$$

$$e_{22} = \sigma_{22}/E_T - \nu_L\sigma_{11}/E_L + [1/2G_L - 1/E_T - \nu_L/E_L](2\sigma_{22}\sin^2\theta + 2\sigma_{12}\cos\theta\sin\theta) + [1/E_T + (1+2\nu_L)/E_L - 1/G_L](\sigma_{11}\cos^2\theta + \sigma_{22}\sin^2\theta + 2\sigma_{12}\cos\theta\sin\theta)\sin^2\theta + [\alpha_T + (\alpha_L - \alpha_T)\sin^2\theta]\Delta T \quad (25)$$

$$e_{12} = \sigma_{12}/2G_L + [1/2G_L - 1/E_T - \nu_L/E_L](\sigma_{11} + \sigma_{22})\cos\theta\sin\theta + [1/E_T + (1+2\nu_L)/E_L - 1/G_L](\sigma_{11}\cos^2\theta + \sigma_{22}\sin^2\theta + 2\sigma_{12}\cos\theta\sin\theta)\cos\theta\sin\theta + [(\alpha_L - \alpha_T)\cos\theta\sin\theta]\Delta T \quad (26)$$

$$e_{33} = -\nu_T/E_T(\sigma_{11} + \sigma_{22}) + [\nu_T/E_T - \nu_L/E_L](\sigma_{11}\cos^2\theta + \sigma_{22}\sin^2\theta + 2\sigma_{12}\cos\theta\sin\theta) + \alpha_T\Delta T \quad (27)$$

Plane Strain:

$$e_{11} = (1-\nu_T^2)\sigma_{11}/E_T - \nu_L(1+\nu_T)\sigma_{22}/E_L +$$
$$[1/2G_L-(1-\nu_T^2)/E_T-\nu_L(1+\nu_T)/E_L](2\sigma_{11}\cos^2\theta + 2\sigma_{12}\cos\theta\sin\theta)$$
$$+ [(1-\nu_T^2)/E_T+[1+2\nu_L(1+\nu_T)-\nu_L\nu_L']/E_L-1/G_L](\sigma_{11}\cos^2\theta$$
$$+ \sigma_{22}\sin^2\theta+2\sigma_{12}\cos\theta\sin\theta)\cos^2\theta$$
$$+ \{(1+\nu_T)\alpha_T + [\alpha_L-(1+\nu_T-\nu_L')\alpha_T]\cos^2\theta\}\Delta T \qquad (28)$$

$$e_{22} = (1-\nu_T^2)\sigma_{22}/E_T - \nu_L(1+\nu_T)\sigma_{11}/E_L +$$
$$[1/2G_L-(1-\nu_T^2)/E_T-\nu_L(1+\nu_T)/E_L](2\sigma_{22}\sin^2\theta + 2\sigma_{12}\cos\theta\sin\theta)$$
$$+ [(1-\nu_T^2)/E_T+[1+2\nu_L(1+\nu_T)-\nu_L\nu_L']/E_L-1/G_L](\sigma_{11}\cos^2\theta$$
$$+ \sigma_{22}\sin^2\theta+2\sigma_{12}\cos\theta\sin\theta)\sin^2\theta$$
$$+ \{(1+\nu_T)\alpha_T + [\alpha_L-(1+\nu_T-\nu_L')\alpha_T]\sin^2\theta\}\Delta T \qquad (29)$$

$$e_{12} = \sigma_{12}/2G_L +$$
$$[1/2G_L-(1-\nu_T^2)/E_T-\nu_L(1+\nu_T)/E_L](\sigma_{11}+ \sigma_{22})\cos\theta\sin\theta +$$
$$[(1-\nu_T^2)/E_T+[1+2\nu_L(1+\nu_T) - \nu_L\nu_L']/E_L-1/G_L](\sigma_{11}\cos^2\theta +$$
$$\sigma_{22}\sin^2\theta+2\sigma_{12}\cos\theta\sin\theta)\cos\theta\sin\theta$$
$$+ \{[\alpha_L-(1+\nu_T-\nu_L')\alpha_T]\cos\theta\sin\theta\}\Delta T \qquad (30)$$

$$\sigma_{33} = \nu_T(\sigma_{11}+\sigma_{22}) - [\nu_T - \nu_L']$$
$$(\sigma_{11}\cos^2\theta+\sigma_{22}\sin^2\theta+2\sigma_{12}\cos\theta\sin\theta)$$
$$- \alpha_T E_T\Delta T \qquad (31)$$

Clearly in order to convert an isothermal plane stress problem into an isothermal plane strain problem, provided n_j is in the plane of isotropy ($n_i d_i = 0$), the following substitutions should be made:

$$E_T = E_T/(1-\nu_T^2)$$

$$E_L = E_L/(1-\nu_L\nu_L') \qquad (32)$$

$$\nu_L = \nu_L(1+\nu_T)/(1-\nu_L\nu_L')$$

where as before

$$\nu_L' = \nu_L E_T/E_L$$

Employing the assumptions of isotropy, i.e. $E=E_T=E_L$ and $\nu=\nu_L=\nu_T$, the above reduce to their isotropic counterparts, as they must. Considering the nonisothermal case, the lack of a unique correspondence in the transverse coefficient of thermal expansion (α_T) is noted when comparing the plane stress and plane strain expressions. This lack of correspondence, arises due to the difference in strain reduction, i.e. poisson ratio, for in plane and out of plane loadings. Clearly however, under isotropic conditions a functional correspondence for the thermal expansion coefficient does exist, i.e. $\alpha = \alpha(1+\nu)$.

Alternatively, the assumptions of plane stress or strain may be imposed out of the plane of isotropy ($n_i d_i \neq 0$). Here, in contrast to the previous assumptions taken in the plane of isotropy, the conversion from a plane stress to a plane strain problem is now a function of fiber orientation, or angle θ. Consider for example the case when $n = (1,0,0)$ and $\theta=0^0$ (i.e. the 1 axis is normal to the plane of isotropy) the following substitutions are required,

$$E_T = E_T/(1-\nu_L\nu_L') \qquad (33)$$

$$\nu_T = (\nu_T + \nu_L\nu_L')/(1-\nu_L\nu_L')$$

while if $\theta=90^0$ (i.e. the 1 axis is in the plane of isotropy) identical substitutions as those in (32) are determined, as expected. For brevity, the angle dependent plane stress and plane strain expressions are omitted here.

EXPERIMENTAL DETERMINATION OF MATERIAL PARAMETERS

Two types of specimens are presumed to be available. These consist of thin walled composite tubes that are longitudinally reinforced (having a single fiber direction oriented axially) and those that are helically reinforced, with a fiber orientation of 45^0 (see figure 4). Each specimen may be loaded either in tension and/or torsion.

The motivation for utilizing thin walled tubular specimens is two fold. The first is the fact that a thin walled tube is an ideal specimen for the development of constitutive relationships as it provides a nearly homogeneous region of stress and strain, and is statically determinate. Secondly, identical specimens may be employed, as well, to characterize inelastic material parameters [3,5] and combined tension/torsion experiments can be used as verification tests to assess the correctness of the multiaxial theory [10], both elastically and inelastically.

First consider the longitudinal reinforced specimen, i.e. $\theta=0^0$, subjected to an axial tensile load (σ_{11}). Clearly, then from equations (24) and (25) we obtain

$$E_L = \sigma_{11}/\epsilon_{11} \tag{34}$$

and

$$\nu_L = -\epsilon_{22}/\epsilon_{11} \tag{35}$$

where σ_{11} is the applied axial stress and $\epsilon_{11}, \epsilon_{22}$ are the measured axial and circumferential strains respectively. Also subjecting the longitudinal specimen to a pure torsional load results in the quantification of the longitudinal shear modulus, as evident from equation (26),

$$G_L = \sigma_{12}/\gamma_{12} \tag{36}$$

where γ_{12} is the measured engineering shear strain ($2\epsilon_{12}$) and σ_{12} the applied torsional stress.

Both the longitudinal and transverse thermal expansion coefficients also may be obtained by imposing a uniform temperature excursion, from some reference temperature, on the longitudinally reinforced specimen. Assuming no additional loads are applied to the specimen, it is easily seen from equations (24) and (25) that

$$\alpha_L = \epsilon^t_{11}/\Delta T$$

and

$$\alpha_T = \epsilon^t_{22}/\Delta T$$

where ΔT is known and ϵ^t_{11} and ϵ^t_{22} are measured quantities.

Now consider the helically reinforced specimen (Fig. 4), with a fiber orientation of 45^0, subjected to a state of pure torsion. Equations (24) thru (27) then simplify to,

$$\epsilon_{11} = \epsilon_{22} = (1/2E_L - 1/2E_T)\sigma_{12} \tag{37}$$

$$\epsilon_{12} = [1/2E_T - (1+2\nu_L)/2E_L]\sigma_{12} \tag{38}$$

and

$$\epsilon_{33} = (\nu_T/E_T - \nu_L/E_L)\sigma_{12} \tag{39}$$

from which the transverse modulus and poisson ratio of the composite material can be deduced. For example, from equations (37) and (39) we obtain

$$E_T = E_L/[1-(2\epsilon_{11}E_L/\sigma_{12})] \tag{40}$$

and

$$\nu_T = E_T(\epsilon_{33}/\sigma_{12} + \nu_L/E_L) \tag{41}$$

while equation (38) allows verification of either E_T,ν_L, or E_L. Note that equation (41) assumes that the radial (diametral) strain (ϵ_{33}) is a measurable quantity. This measurement, however, is at best difficult. Clearly, if this measurement proves to elusive, an alternative test will need to be conducted to determine either the transverse shear modulus (G_T) or the transverse poisson ratio (ν_T). As an example, the double shear test may be employed to obtain a measure of the transverse shear modulus [11].

Although, the author prefers the use of tubular specimens, the high cost of fabrication and required test equipment may be prohibitive. Thus alternative test procedures, utilizing plate specimens may also be employed to obtain the required independent material parameters. The four material parameters E_L,E_T, ν_L and ν_T can be obtained by performing tensile tests on plate specimens with orientations of 0 and 90^0, see figure 5. Difficulties arise however, when attempting to find G_L, as in–plane shear test methods must be employed; such as rail shear, symmetric rail shear, $\pm$ 45^0 tension coupon, off axis tensile coupon, ARCAN and IOSIPESCU. The symmetric rail shear and $\pm$ 45^0 tension coupon appear to be the preferred methods [12].

Finally, it is important to realize that although the above tests are viewed as *characterization* tests for the present theory, they also may be viewed as *verification* tests for the various micromechanics theories.

RESTRICTIONS ON THE MATERIAL PARAMETERS

Theoretical constraints, which insure the admissibility of the elastic constants incorporated in the above expressions,
may be derived by requiring that the complementary energy (strain energy) potential be positive definite; thereby guaranteeing convexity and uniqueness of solution. These inequalities are

$$\begin{aligned} &E_L > 0 \\ &G_L > 0 \\ &G_T > 0 \\ &E_L/E_T > \nu_L^2 \\ &1-\nu_T > 2\nu_L^2 E_T/E_L \end{aligned} \tag{42}$$

Under isotropic conditions (i.e. $E=E_L=E_T$, $G=G_L=G_T$ and $\nu=\nu_L=\nu_T$) these inequalities simplify to the well known restrictions imposed on elastic isotropic materials [6].

An additional restriction is imposed on the longitudinal shear modulus which insures that the global longitudinal (transverse) stiffness modulus be monotonically decreasing (increasing) for all fiber orientations between zero and ninety degrees. The necessary inequality is

$$G_L \leq E_L/[2(1+\nu_L)] \tag{43}$$

and may be deduced from either of the following conditions:

$$dE_{11}/d\theta = 4\epsilon_{12}\sigma_{11}/\epsilon_{11}^2 < 0 \tag{44}$$

or

$$dE_{22}/d\theta = -4\epsilon_{12}\sigma_{22}/\epsilon_{22}^2 > 0 \tag{45}$$

where E_{11},E_{22} are the global longitudinal and transverse stiffness moduli respectively and ϵ_{11},ϵ_{22} and ϵ_{12} are given by equations (24) thru (26).

Figures 6 and 7 illustrate the resulting variation in stiffness (for sample material 1 and 2, respectively) along the 1 axis with respect to fiber orientation when the inequality of equation (43) is violated and satisfied, respectively. Table 1 provides the two complete sets of example material properties. Clearly, when G_L violates (43) a non realistic variation in stiffness, with respect to fiber orientation, results (see figure 5). The increase

and subsequent decrease in stiffness is attributed to the change in sign of the shear strain, as illustrated in figure 8, and implied in (44). In figure 8, the corresponding normal and shear strain variations verses fiber orientation are displayed, utilizing the material properties of sample one. Alternatively, figure 9 shows the normal and shear strain variations associated with the material parameters of sample two, i.e. figure 7. Also the importance of the sign, as well as magnitude, of the shear strain, i.e. ϵ_{12}, is evident from the expressions (44) and (45).

The inequalities in equations (42) and (43) not only constrain the values of the elastic constants in the mathematical formulation to agree with certain basic physical principles, but also provide a means to determine whether experimentally obtained data is physically consistent with the mathematical model. If the measured material properties satisfy the constraints, one can proceed with confidence. Otherwise one might doubt the experimental techniques employed; or alternatively, the validity of the assumed idealization of transversely isotropic behavior for this particular material.

SIMPLE ILLUSTRATIVE STATES OF STRESS

Simple homogeneously stressed elements are employed in this section to illustrate the effect of fiber orientation on the resulting strain distributions. All results are associated with the material properties of sample 2 in Table 1. Four mechanical stress states and one thermal load are addressed. These are a uniaxial state, a pure shear state, an equal and opposite biaxial state, a two to one biaxial state, and a change in temperature with no applied stress. The resulting variations in strain with fiber orientation are shown in figures 9 thru 13, respectively.

Examination of these figures reveals that the strain response , as one might expect, is highly dependent upon fiber orientation. Further, qualitative agreement with physical reasoning and experimentally observed response is also noted, thus providing additional confidence in the correctness of the present thermoelastic stress–strain relations. For example, consider the uniaxial stress state of figure 9. There the ϵ_{11} strain component is seen to be extensional (positive) for all fiber orientations, while ϵ_{22} is initially contractive (negative, e.g. at θ=0^0) yet reaches a maximum extensional magnitude at θ=45^0. This change in sign for the ϵ_{22} strain component would be completely unanticipated if one applied intuition developed from isotropic materials. Additionally no contraction or extension along the 2 axis would be observed when the fibers are orientated at either θ= 17.05^0 or 72.95^0, see figure 9. Such points of interest may be examined experimentally to verify the theory.

Examining figures 10 and 11 (the pure shear and equal and opposite biaxial stress state, respectively) one must realize that although the strain responses appear to be distinct, they are in fact equivalent; as expected since the applied stress states are equivalent, provided the proper transformation is applied. For example with a rotation of 45^0, the biaxial stress state of figure 11, becomes one of pure shear, thus suggesting that the strain response be equivalent to that of figure 10 at $\theta=0^0$. Indeed, taking into account a 45^0 transformation, this can be easily shown to be the case.

Consider the two to one biaxial stress state given in figure 12. This stress state is similar to that which arises in a thin walled tube with closed ends under internal pressure. As expected, the hoop strain (ϵ_{22}) is significantly larger than the axial strain (ϵ_{11}) at $\theta=0^0$ (a longitudinally reinforced tube). Increasing the fiber orientation toward 90^0 (i.e. circumferentially reinforced) decreases the hoop strain while increasing the axial. Interestingly, beyond 55^0 (a material dependent angle measurement) the magnitude of the axial strain surpasses that of the hoop strain, where at 90^0 ϵ_{11} is approximately twice that of ϵ_{22}, even though $\sigma_{22} = 2\sigma_{11}$. One obvious application of the present theory is the optimization of fiber orientation, such that specific design criteria are satisfied. Adoption of known optimization principles to the present theory is straight forward: due to the inclusion of directional dependence (material symmetry) in the potential function.

The effect of fiber orientation on the variation in thermal strains is illustrated in figure 13. Unlike the isotropic case, here a change in temperature may produce (for off axis fiber orientations) significant shear strains in addition to volumetric strains. The maximum shear strain, under a purely thermal load, will always occur at an angle of 45^0, independent of material constants.

SUMMARY

A continuum theory has been presented that represents the linear thermoelastic behavior of materials which can be idealized as transversely isotropic. Specifically this theory may be applied to composite materials with a single preferred direction; wherein the composite is considered a material in its own right, with its own experimentally measurable properties specified for the composite as a whole.

Some of the main points of the present study are:

1) The present theory is shown to be in agreement with earlier work done by Spencer, Lekhnitskii, and Chadwick and Seet. Also, assuming isotropic conditions, the present theory is shown to simplify to the classical thermoelastic stress–strain relations.

2) Correspondence between isothermal plane stress and plane strain problems was established, while for the assumed multiaxial form of the thermal strain no correspondence is found for the nonisothermal case.

3) Specification of an experimental procedure for the complete determination of the required material parameters is presented. Thin walled tubes, longitudinally and helically reinforced, loaded in tension and torsion are the primary specimens.

4) Theoretical constraints on the values of the elastic constants, which insure their admissibility, are discussed.

5) Simple illustrative states of stress indicate that the resulting strain response, in the presence of material anisotropy, may be highly nonintuitive.

REFERENCES

1) Agarwal, B.D. and Broutman, L.J., Analysis and Performance of Fiber Composites, John Wile & Sons, 1980.

2) Spencer, A.J.M., Deformations of Fiber–Reinforced Materials, Claremont Press, Oxford, 1972.

3) Robinson,D.N. and Duffy, S.F., "A Continuum Deformation Theory for Metal–Matrix Composites at High Temperature", to appear Jnl. Mech Phys. and Solids.

4) Spencer, A.J.M., Continuum Theory of the Mechanics of Fiber–Reinforced Composites, Springer–Velag, 1984.

5) Robinson, D.N., Duffy S.F. and Ellis, J.R., " A Viscoplastic Constitutive Theory for Metal Matrix Composites at High Temperature", Thermal Stress, Material Deformation, and Thermo–Mechanical Fatigue, Ed. by Sehitoglu H. and Zamrik S.Y., ASME, PVP, Vol 123, 1987.

6) Chen W.F. and Saleeb A.F., Constitutive Equations for Engineering Materials, Vol I – Elasticity and Modeling, John Wiley & Sons, 1982.

7) Spencer, A.J.M., "Theory of Invariants", In Continuum Physics, Ed. Eringen A. C., Academic Press, Vol I, pp 240–355, 1971.

8) Lekhnitskii, S.G., Theory of Elasticity of an Anisotropic Body, Holden–Day, San Francisco, 1963.

9) Chadwick, P. and Seet L.C.T., "Second–order Thermoelasticity Theory for isotropic and transversely isotropic materials", In Trends in Elasticity and Thermoelasticity, Eds. Czarnota–Bojarski R.E.,Sokolowski M. and Zorski H., Wolters–Noordhoff, Groningen, pp29–57, 1971.

10) Robinson,D.N. and Ellis J.R., "Experimental Determination of Flow Potential Surfaces Supporting a Multiaxial Formulation of Viscoplasticity", Proc. 5th International seminar on Inelastic Analysis and Life Prediction in High Temperature Environments, Paris, France, 1985.

11) Schwartz,D.M., Mitchell, J.B. and Dorn J.E., "The Mechanism of Prismatic Creep in Mg–12 at %Li ", ACTA Metallurgica, Vol 15, March 1967.

12) Dvorak G. J. and Zweben C., "Metal and Ceramic Matrix Composites", Short Course, UCLA, Winter 1987.

APPENDIX – MATRIX REPRESENTATION OF MULTIAXIAL FORMULATION

The multiaxial stress–strain relations given in index notation in equations (9) and (10) are expanded and expressed here in matrix notation. This is done in order to simplify and accelerate implementation of the present theory into structural analysis codes. Equations (9) and (10) now become

$$\{\sigma\} = [C]\ \{\epsilon\} \qquad \text{(a)}$$

and

$$\{\epsilon\} = [D]\ \{\sigma\} \qquad \text{(b)}$$

respectively. Where the column matrices $\{\sigma\}$ and $\{\epsilon\}$ contain the six independent tensorial components of σ_{ij} and ϵ_{ij}. That is

$$\{\sigma\} = [\sigma_{11},\sigma_{22},\sigma_{33},\sigma_{12},\sigma_{23},\sigma_{31}]^T$$

and

$$\{\epsilon\} = [\epsilon_{11},\epsilon_{22},\epsilon_{33},\epsilon_{12},\epsilon_{23},\epsilon_{31}]^T$$

Note the inclusion of thermal strains,in the above equations, is accomplished by utilizing equation (22), i.e. substituting

$$\epsilon_{ij} = e_{ij} - \epsilon^t_{ij}$$

into equations (a) and (b).

The independent components of the symmetric stiffness matrix, [C], are now expressed in terms of the nonphysical parameters as follows:

First Row:

$$C_{11} = 2A'/9 + B'/2 + [2C'-B'+2E'/3]d_1^2 + [B'/2 + 2(D'-C')]d_1^4$$

$$C_{12} = 2A'/9 - B'/2 + [B'/2 +E'/3](d_1^2+d_2^2) + [B'/2 + 2(D'-C')]d_1^2d_2^2$$

$$C_{13} = 2A'/9 - B'/2 + [B'/2 +E'/3](d_1^2+d_3^2) + [B'/2 + 2(D'-C')]d_1^2d_3^2$$

$$C_{14} = [C'-B'/2+E'/3]d_1d_2 + [B'/2 + 2(D'-C')]d_1^3d_2$$

$$C_{15} = [B'/2+E'/3]d_2d_3 + [B'/2 + 2(D'-C')]d_1^2d_2d_3$$

$$C_{16} = [C'-B'/2+E'/3]d_1d_3 + [B'/2 + 2(D'-C')]d_1^3d_3$$

Second Row:

$$C_{22} = 2A'/9 + B'/2 + [2C'-B'+2E'/3]d_2^2 + [B'/2 + 2(D'-C')]d_2^4$$

$$C_{23} = 2A'/9 - B'/2 + [B'/2 +E'/3](d_3^2+d_2^2) + [B'/2 + 2(D'-C')]d_2^2d_3^2$$

$$C_{24} = [C'-B'/2+E'/3]d_1d_2 + [B'/2 + 2(D'-C')]d_2^3d_1$$

$$C_{25} = [C'-B'/2+E'/3]d_2d_3 + [B'/2 + 2(D'-C')]d_2^3d_3$$

$$C_{26} = [B'/2+E'/3]d_1d_3 + [B'/2 + 2(D'-C')]d_2^2d_3d_1$$

Third Row:

$$C_{33} = 2A'/9 + B'/2 + [2C'-B'+2E'/3]d_3^2 + [B'/2 + 2(D'-C')]d_3^4$$

$$C_{34} = [B'/2+E'/3]d_1d_2 + [B'/2 + 2(D'-C')]d_3^2d_2d_1$$

$$C_{35} = [C'-B'/2+E'/3]d_2d_3 + [B'/2 + 2(D'-C')]d_3^3d_2$$

$$C_{36} = [B'/2+E'/3]d_1d_3 + [B'/2 + 2(D'-C')]d_3^3d_1$$

Fourth Row:

$$C_{44} = B' + [C'-B'](d_1^2 + d_2^2) + [B'/2 + 2(D'-C')]d_1^2 d_2^2$$

$$C_{45} = [C'-B']d_1 d_3 + [B'/2 + 2(D'-C')]d_1 d_2^2 d_3$$

$$C_{46} = [C'-B']d_2 d_3 + [B'/2 + 2(D'-C')]d_1^2 d_2 d_3$$

Fifth Row:

$$C_{55} = B' + [C'-B'](d_2^2 + d_3^2) + [B'/2 + 2(D'-C')]d_2^2 d_3^2$$

$$C_{56} = [C'-B']d_1 d_2 + [B'/2 + 2(D'-C')]d_1 d_2 d_3^2$$

Sixth Row:

$$C_{66} = B' + [C'-B'](d_1^2 + d_3^2) + [B'/2 + 2(D'-C')]d_1^2 d_3^2$$

The components of the compliance matrix, [D], are identical to those above, provided the unprimed coefficients A,B,C,D and E are substituted for their primed counterparts. For convenience the definitions of these nonphysical parameters, in terms of the more physical parameters, are repeated (c.f. equations (18) and (19)).

The unprimed coefficients are

$$A = 9/4[(1-\nu_T)/E_T]$$

$$B = 1/2G_T$$

$$C = 1/2G_L \qquad (c)$$

$$D = (1+2\nu_L)/2E_L + (1-\nu_T)/4E_T$$

$$E = -3\{ (1-\nu_T)/2E_T + \nu_L/E_L \}$$

where

$$2G_T = E_T/(1+\nu_T)$$

$$\nu_L' = \nu_L E_T/E_L$$

and the primed are

$$A' = 9/4\left\{E_T E_L/[E_L(1-\nu_T) - 2E_T\nu_L^2]\right\}$$

$$B' = 2G_T$$

$$C' = 2G_L \qquad \text{(d)}$$

$$D' = E_L\{1 + E_T(1-2\nu_L)^2/[2(E_L(1-\nu_T)-2E_T\nu_L^2)]\}/2$$

$$E' = -3\{E_T E_L(1-2\nu_L)/[E_L(1-\nu_T)-2E_T\nu_L^2]\}/2$$

Table 1

material	E_L (in ksi)	E_T (in ksi)	G_L (in ksi)	ν_L	ν_T	α_L ($\times 10^{-6}$)	α_T ($\times 10^{-6}$)
sample 1	28000	13000	18000	0.25	0.35	15.0	3.0
sample 2	50000	13000	15000	0.25	0.35	15.0	3.0

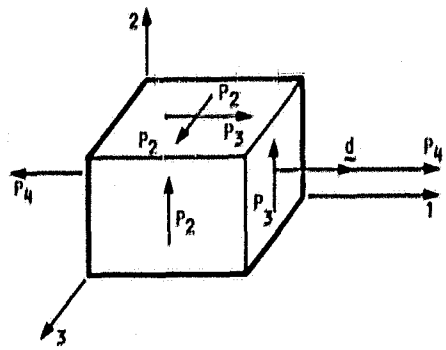

FIGURE 1. - DEFINITION OF COORDINATE SYSTEM AND PHYSICAL INVARIANTS WITH RESPECT TO THE PREFERRED FIBER DIRECTION $\underline{d}$.

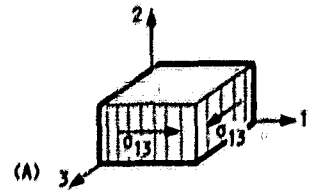

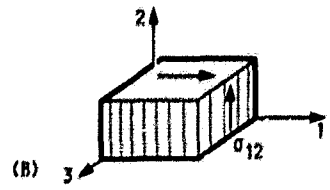

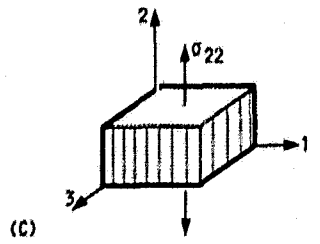

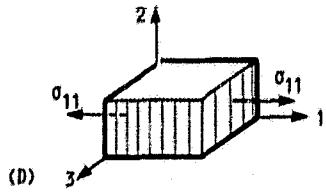

FIGURE 2. - FUNDAMENTAL STRESS STATES, WITH RESPECT TO A GIVEN FIBER DIRECTION, REQUIRED TO DETERMINE MATERIAL PARAMETERS.

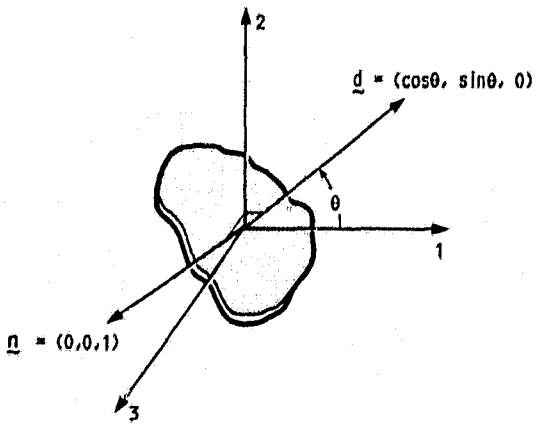

FIGURE 3. - DEFINITION OF COORDINATE SYSTEM AND PLANE OF ISOTROPY.

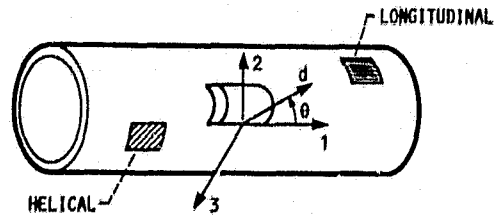

FIGURE 4. - SCHEMATIC OF A THIN WALLED COMPOSITE TUBE LONGITUDINALLY ($\theta = 0^{o}$) AND HELICALLY (E.G. $\theta = 45^{o}$) REINFORCED.

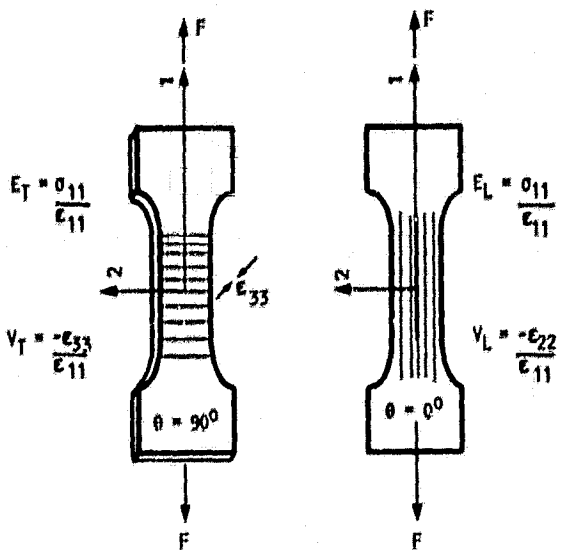

FIGURE 5. - SCHEMATIC OF PLATE SPECIMENS LONGITUDINALLY ($\theta = 0^0$) AND TRANSVERSELY ($\theta = 90^0$) REINFORCED.

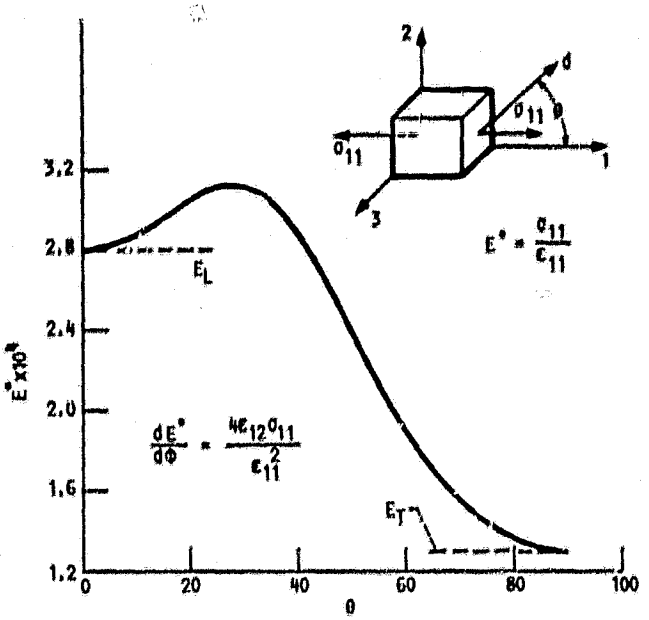

FIGURE 6. - VARIATION IN STIFFNESS (E_{11}) WITH RESPECT TO FIBER ORIENTATION θ ASSUMING SAMPLE 1 (SEE TABLE 1) MATERIAL PARAMETERS.

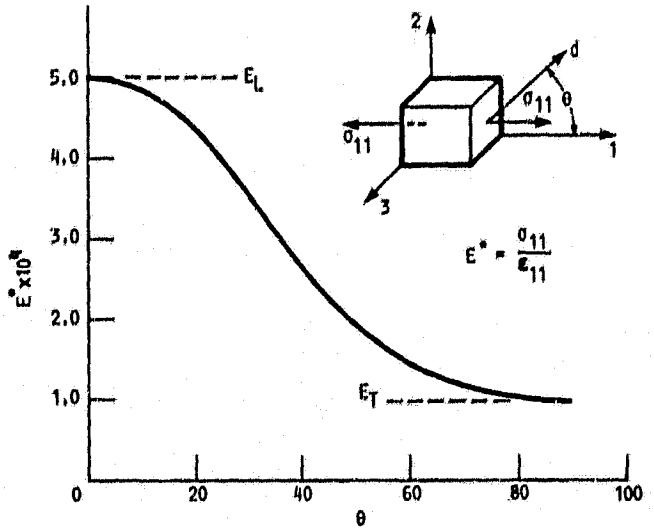

FIGURE 7. - VARIATION IN STIFFNESS (E_{11}) WITH RESPECT TO FIBER ORIENTATION θ ASSUMING SAMPLE 2 (SEE TABLE 1) MATERIAL PARAMETERS.

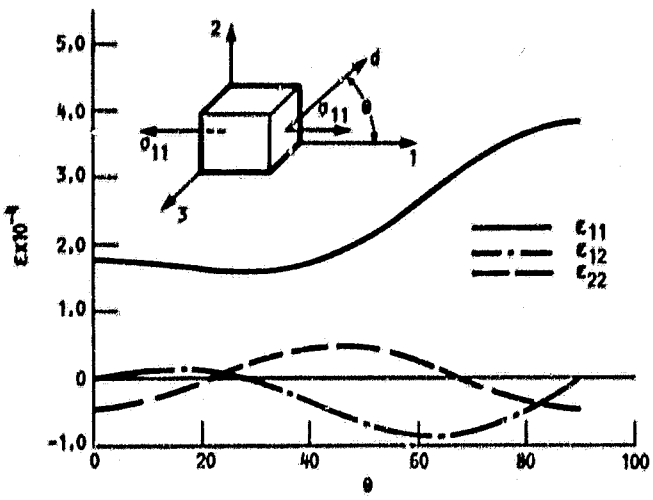

FIGURE 8. - NORMAL (ε_{11}, ε_{22}) AND SHEAR (ε_{12}) STRAIN VARIATION VERSUS FIBER ORIENTATION θ ASSUMING SAMPLE 1 MATERIAL PARAMETERS.

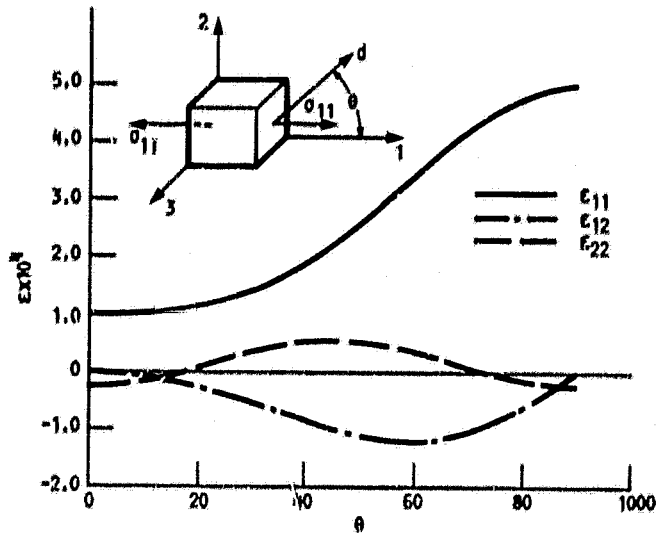

FIGURE 9. - NORMAL (ε_{11}, ε_{22}) AND SHEAR (ε_{12}) STRAIN VARIATION VERSUS FIBER ORIENTATION θ ASSUMING SAMPLE 2 MATERIAL PARAMETERS.

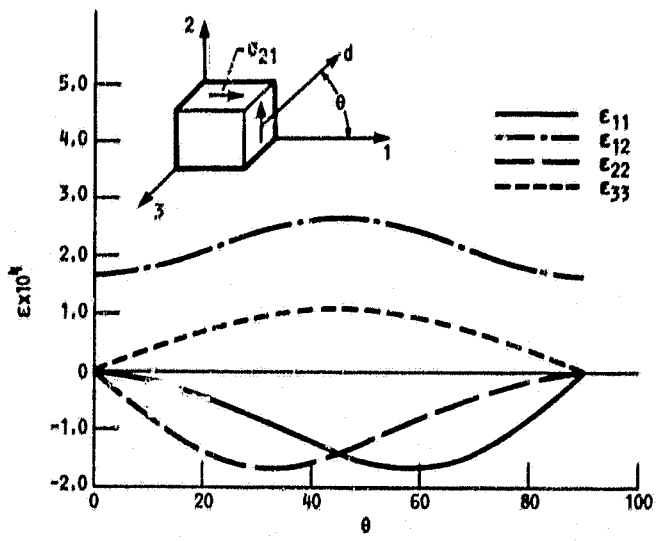

FIGURE 10. - NORMAL (ε_{11},ε_{22},ε_{33}) AND SHEAR (ε_{12}) STRAIN VARIATION VERSUS FIBER ORIENTATION θ FOR SAMPLE 2 MATERIAL PARAMETERS UNDER PURE SHEAR STRESS STATE.

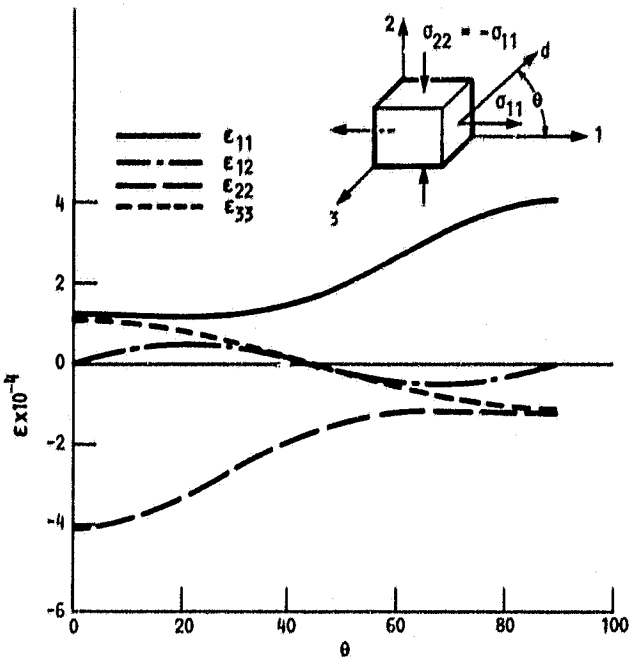

FIGURE 11. - NORMAL (ε_{11},ε_{22},ε_{33}) AND SHEAR (ε_{12}) STRAIN VARIATION VERSUS FIBER ORIENTATION θ FOR SAMPLE 2 MATERIAL PARAMETERS UNDER OPPOSITE BIAXIAL STRESS STATE.

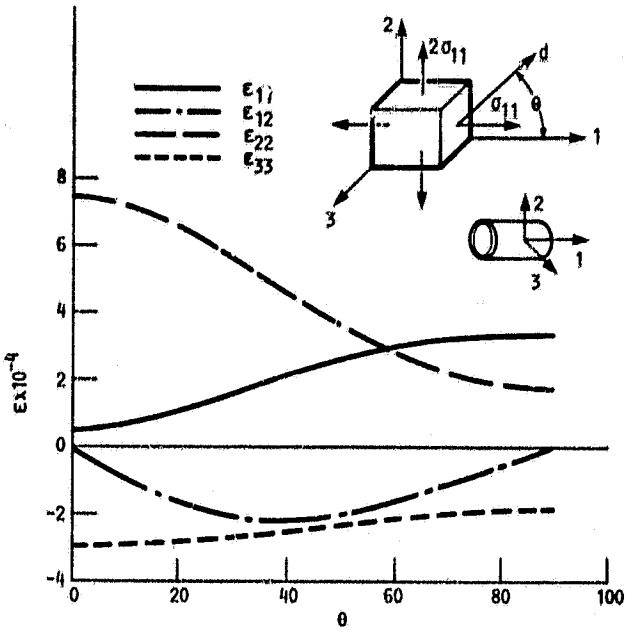

FIGURE 12. - NORMAL (ε_{11},ε_{22},ε_{33}) AND SHEAR (ε_{12}) STRAIN VARIATION VERSUS FIBER ORIENTATION θ FOR SAMPLE 2 MATERIAL PARAMETERS UNDER TWO TO ONE BIAXIAL STRESS STATE.

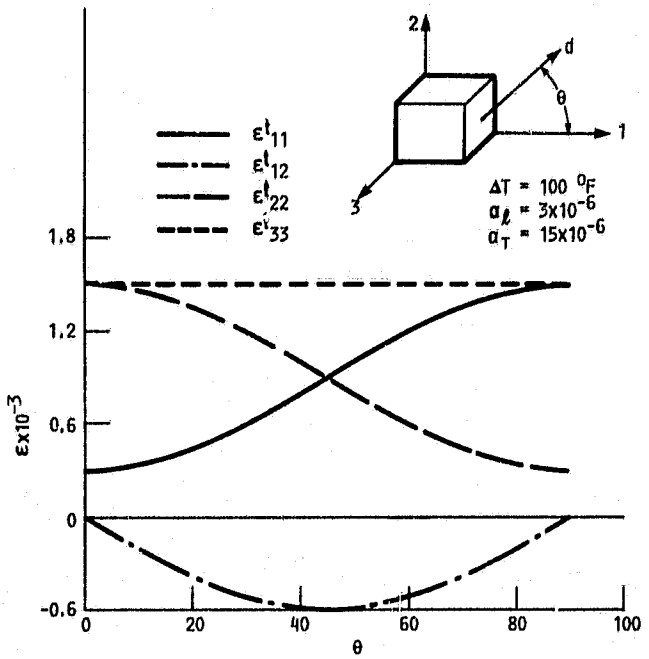

FIGURE 13. NORMAL (ε^t_{11},ε^t_{22},ε^t_{33}) AND SHEAR (ε^t_{12}) STRAIN VARIATION VERSUS FIBER ORIENTATION θ FOR SAMPLE 2 MATERIAL PARAMETERS FOR A CHANGE IN TEMPERATURE $\Delta T = 100\ ^oF$.

NASA
National Aeronautics and Space Administration

Report Documentation Page

1. Report No.	2. Government Accession No.	3. Recipient's Catalog No.
NASA TM-101302 *Corrected Copy*		

4. Title and Subtitle
A Transversely Isotropic Thermoelastic Theory

5. Report Date
November 1989

6. Performing Organization Code

7. Author(s)
S.M. Arnold

8. Performing Organization Report No.
E-4288

10. Work Unit No.
535-07-01

9. Performing Organization Name and Address
National Aeronautics and Space Administration
Lewis Research Center
Cleveland, Ohio 44135-3191

11. Contract or Grant No.

13. Type of Report and Period Covered
Technical Memorandum

12. Sponsoring Agency Name and Address
National Aeronautics and Space Administration
Washington, D.C. 20546-0001

14. Sponsoring Agency Code

15. Supplementary Notes

16. Abstract

A continuum theory is presented for representing the thermoelastic behavior of composites that can be idealized as transversely isotropic. This theory is consistent with anisotropic viscoplastic theories being developed presently at NASA Lewis Research Center. A multiaxial statement of the theory is presented, as well as plane stress and plane strain reductions. Experimental determination of the required material parameters and their theoretical constraints are discussed. Simple homogeneously stressed elements are examined to illustrate the effect of fiber orientation on the resulting strain distribution. Finally, the multiaxial stress-strain relations are expressed in matrix form to simplify and accelerate implementation of the theory into structural analysis codes.

17. Key Words (Suggested by Author(s))	18. Distribution Statement
Elasticity Transverse isotropy Composites Thermal strain	Unclassified – Unlimited Subject Category 39

19. Security Classif. (of this report)	20. Security Classif. (of this page)	21. No of pages	22. Price*
Unclassified	Unclassified	28	A02

*For sale by the National Technical Information Service, Springfield, Virginia 22161